Estimation of broadband emissivity from satellite multi-channel thermal infrared data using spectral libraries

K. Ogawa, Thomas Schmugge, Frederic Jacob, Andrew French

Estimation of Broadband Emissivity from Satellite Multi-Channel Thermal Infrared Data Using Spectral Libraries

Kenta Ogawa*+, Thomas Schmugge*, Frederic Jacob* and Andrew French*

*USDA/ARS Hydrology and Remote Sensing Lab: Beltsville, MD 20705-2350
+Hitachi Ltd.: Tokyo, 101-8010, Japan
E-mail: kenta@hydrolab.arsusda.gov

***Abstract*- Surface broadband thermal infrared emissivity is an important parameter for estimating the longwave surface energy balance. This study focuses on estimating the broadband emissivity from the emissivities of the five channels on the Advanced Spaceborne Thermal Emission and Reflection Radiometer / Thermal Infrared Radiometer (ASTER/TIR). ASTER is a sensor onboard the Earth Observing System (EOS) Terra satellite launched in 1999, and has five channels in the thermal infrared region (8-12 µm). Using this sensor, it is possible to estimate surface spectral emissivity for each channel at a spatial resolution of 90 m.**

Broadband emissivities (3-14 µm) were calculated using two spectral libraries, John Hopkins University Spectral Library (JHU Library) and MODIS UCSB (University of California, Santa Barbara) Emissivity Library (UCSB Library). They ranged from 0.89 to 0.99 for natural surfaces, such as, rocks, soils, vegetation, water, ice, and snow. Then, we assumed that the broadband emissivity can be expressed as a linear combination emissivities for the five ASTER/TIR channels. The linear regression was calibrated using JHU Library and validated with the UCSB Library. The absolute error on the estimated broadband emissivity was less than 0.01 for 93 % of all samples and RMSE was 0.0051 over an emissivity range from 0.91 to 0.99 in validation.

Finally, this calibrated regression was applied to emissivities computed from the data acquired with ASTER/TIR over the Jornada Experimental Range in New Mexico to produce a map of broadband emissivity for this area.

I. INTRODUCTION

Surface broadband emissivity is an important parameter for estimating the longwave surface energy. Mostly, the broadband emissivity may vary significantly, because the spectral emissivity variation ranges from 0.7 to 1.0 for bare soils and rocks (see Fig. 1) in the 8-12 µm range, there is smaller variation in the 5-8 µm and 12-14 µm ranges.

A constant emissivity is often used for land surface in energy balance study and general circulation models (GCMs). But, the spatial variation of broadband emissivity may cause a feedback and affect surface temperature in GCMs.

Recent spaceborne thermal infrared multispectral sensors, such as ASTER, allow the estimation of spectral emissivities from local to global scales. We are helped in this effort by the fact that the peak in the thermal emission is at ~10 µm, i.e. the region we have measurements.

In this study, we propose to express the broadband emissivity as a linear combination of channel emissivities of ASTER/TIR. Firstly, we produced a dataset of the broadband emissivity (3-14 µm), and channel emissivities for ASTER/TIR, using spectral libraries. Then we calibrate and validate a regression using the dataset. Finally, we computed broadband emissivities over the Jornada Experimental Range [1], New Mexico with ASTER/TIR using the calibrated regression.

II. METHOD & DATA

Broadband emissivity is defined in (1):

$$\varepsilon_{\lambda 1-\lambda 2} \equiv \frac{\int_{\lambda=\lambda 1}^{\lambda=\lambda 2} \varepsilon(\lambda)\,\mathrm{B}(\lambda,T)\,d\lambda}{\int_{\lambda=\lambda 1}^{\lambda=\lambda 2} \mathrm{B}(\lambda,T)\,d\lambda} \qquad (1).$$

Where ε is surface thermal infrared emissivity, λ is the wavelength, B is the Planck function, and T is surface temperature. In this study, we selected a wavelength range, λ_1=3.3 µm to λ_2=14.0 µm, since spectral libraries covered this wavelength range. We assume T = 300 K in this analysis. We computed the difference of broadband emissivity caused by variation of target temperature. It was smaller than 0.005 over the range from 270 K to 330 K. We note that the emission at wavelengths longer than 14 µm is about 40 % to 50 % of the total blackbody radiation and that we have no spectral emissivity data of these longer wavelengths.

AS5TER channel emissivity ε_{ch} is defined in (2) as:

$$\varepsilon_{ch} \equiv \frac{\int_{\lambda=\lambda 1}^{\lambda=\lambda 2} f_{ch}(\lambda)\varepsilon(\lambda)\,\mathrm{B}(\lambda,T)\,d\lambda}{\int_{\lambda=\lambda 1}^{\lambda=\lambda 2} f_{ch}(\lambda)\,\mathrm{B}(\lambda,T)\,d\lambda} \qquad (2).$$

Where f_{ch} is the spectral response function of ASTER/TIR channel.

We assume that broadband emissivity can be expressed in (3) as:

$$\varepsilon_{3.3-14.0} = \sum_{ch=10}^{14} a_{ch}\varepsilon_{ch} + c \qquad (3).$$

The center wavelengths of ASTER channel 10 to 14 are

8.3, 8.65, 9.1, 10.6, 11.3 μm, respectively. Then we calibrate and validate the coefficients of (3) using two spectral libraries.

We used two spectral libraries; One is those collected by Jack Salisbury of Johns Hopkins University (JHU Library) [2] and the other is collected by University of California Santa Barbara (UCSB Library) [3]. We selected 150 samples spectra from the JHU Library including soils, vegetation, rock (except fine powders), water, and ice emissivity spectra, and selected 107 samples spectra from UCSB library including soils, vegetation, and water.

The JHU library contains directional hemispherical spectral reflectance, ρ_λ, therefore we converted to spectral emissivity ε_λ using Kirchhoff's law, $\varepsilon_\lambda=1-\rho_\lambda$. The spectra of the fine powdered samples (particle size: <50 μm) were not used in this study, because they may not follow this relation [4].

ASTER data were acquired on 12 May 2001 over the Jornada Experimental Range in New Mexico, a desert grassland where the main vegetation components are grass and shrubs. The data were atmospherically corrected using MODTRAN with NCEP atmospheric profiles. Then the MMD method [5] was applied to separate the surface temperature and spectral emissivity from surface spectral radiance.

III. RESULTS

A. Spectral libraries and broadband emissivity

Fig. 1 displays the average and range of spectral emissivity for data from both libraries. The range is larger both over [3 – 5] μm and [8 – 10] μm regions than in other wavelength regions. Because the emitted energy is low over 3 to 5 μm at around 300 K, it is expected that the emissivity from 8 to 10 μm (ASTER channel 10, 11, 12) will strongly affect the broadband emissivity.

The calculated broadband emissivities range from 0.885 to 0.994. Mean emissivity of rock, soil, vegetation, and water is 0.938, 0.955, 0.967, and 0.982 respectively.

B. Calibration & Validation

Table I displays the calibrated coefficients of computed from the step-wise regression. The coefficient of 0.0 for channel 13 (a_{13}) means that the variable was dropped, because it was not statistically significant. Table II shows the range of emissivity, and RMSE and maximum error. RMSE is smaller than 0.01. The error was large in some kinds of igneous rocks, especially in ultramafic and mafic rocks samples, such as picrite. Maximum absolute error is 0.023.

Table III shows RMSE, maximum error, and range of emissivity for validation with UCSB library. The agreement between estimated broadband emissivity and calculated ones is consistent. The difference was smaller than 0.01 for 100 of 107 samples (93%).

Figure 2 shows the comparison of the estimated broadband emissivity against the calculated value using spectral libraries. We noticed an underestimation for the samples with higher emissivity (around 0.99), such as vegetation and water. This may results, because of the small number of spectra for these types ain the calibration. We also tried other empirical functions, such as, 1) the linear regression without a constant, and 2) polynomial regression. But we didn't observe significant improvements in either instance.

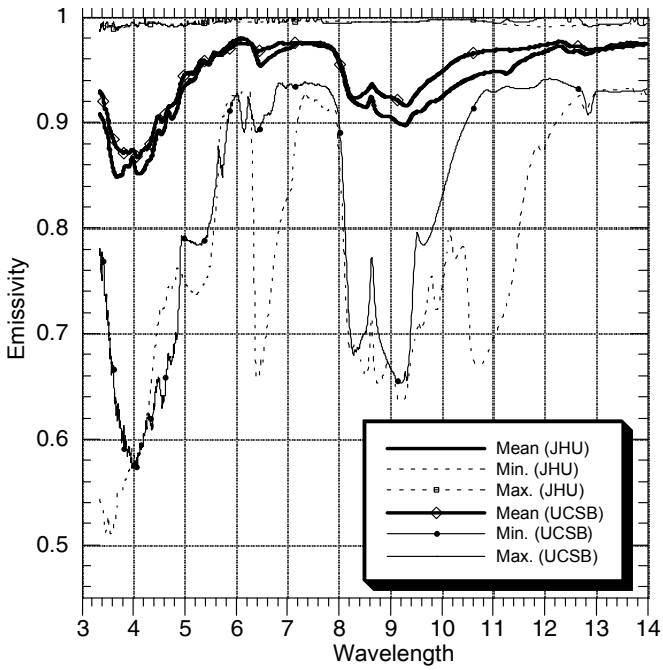

Fig. 1. The mean and range of emissivity in spectral libraries samples.

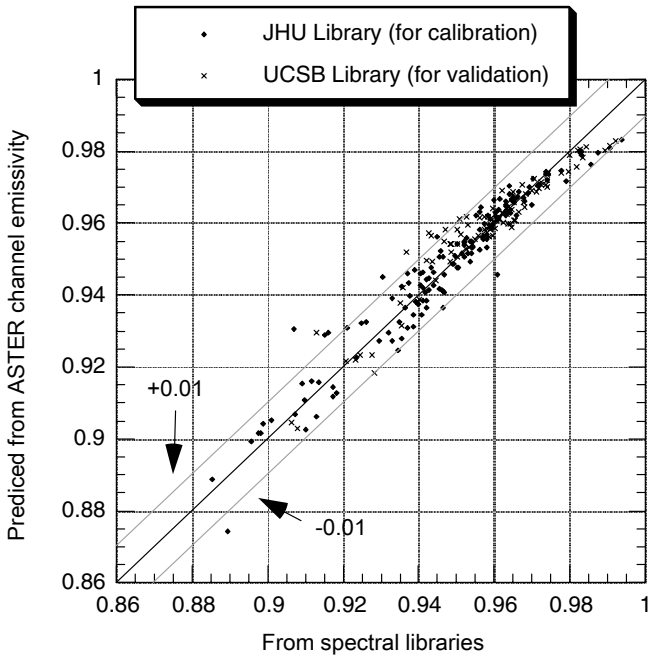

Fig. 2. Predictions of broadband emissivity.

Table I
Calibrated coefficients computed using JHU Library

a_{10}	a_{11}	a_{12}	a_{13}	a_{14}	c
0.035	0.072	0.118	0.000	0.381	0.380

Table II
The error and range of broadband emissivity in calibration

RMSE	Maximum error	Range
0.0055	0.023	0.885-0.994

Table III
The error and range of broadband emissivity in validation

RMSE	Maximum error	Range
0.0051	0.016	0.906-0.992

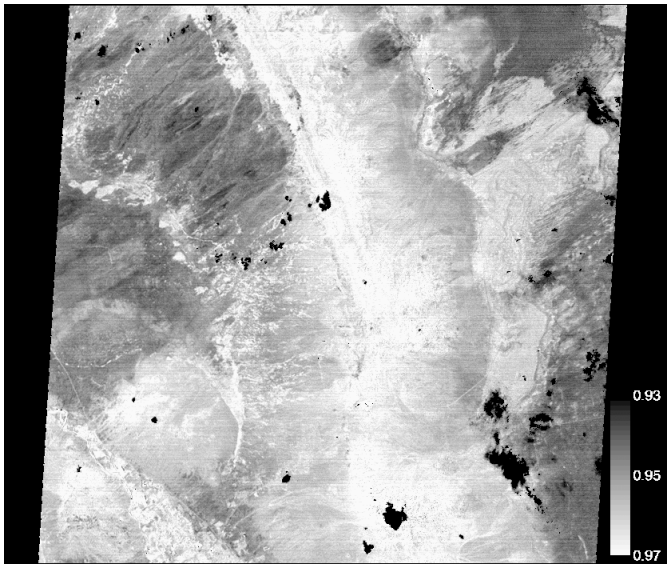

Fig. 3 Broadband emissivity map of Jornada Experimental Range.

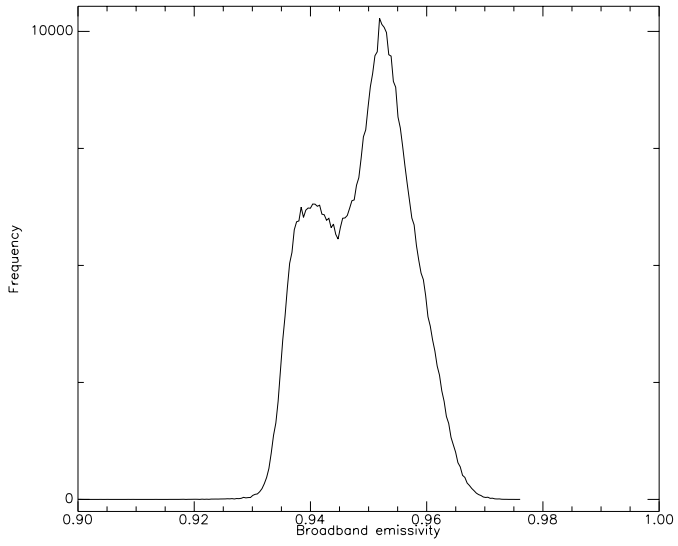

Fig. 4 Histogram of broadband emissivity for Jornada site.

C. Application to ASTER data

This calibrated regression was finally applied to emissivities computed from ASTER/TIR data acquired over the Jornada Experimental Range in New Mexico. The result is shown in Fig. 3. The histogram of extracted emissivities is shown in Fig. 4. Emissivities range from 0.93 to 0.97 with the average ~0.95.

In Fig. 3, the bright area in the upper center to lower center of the image corresponds to a ridge with vegetation. Another bright area in lower left corresponds to agricultural fields along the Rio Grande River. These areas have higher emissivities range from 0.96 to 0.97.

The darker area at upper left and right edge is bare soil or sparsely vegetated sites. The upper right area is for the gypsum at white sand. These areas have lower emissivities that range from 0.93 to 0.95.

IV. SUMMARY AND CONCLUSIONS

The results of the spectral libraries analysis suggest that the estimation of broadband emissivity of 3-14 μm using the linear regression from emissivities of ASTER/TIR channels is potentially accurate and the expected RMSE is lower than 0.01 for the emissivity range from 0.90 to 0.99.

The estimated broadband emissivity using the regression in Jornada site showed the variation of 0.04, from 0.93 to 0.97.

ACKNOWLEDGMENTS

This study was supported by the ASTER Project of NASA's EOS-Terra Program.

REFERENCES

[1] T. Schmugge, A. French, J.C. Ritchie, A. Rango, and H. Pelgrum, "Temperature and emissivity separation from multispectral thermal infrared observations, *Remote Sensing of Environment*, vol. 79, pp. 189-198, 2002.

[2] J.W. Salisbury and D.M. D'Aria, "Emissivity of terrestrial materials in the 8-14 μm atmospheric window", *Remote Sensing of Environment*, vol. 42, pp. 83-106, 1992.

[3] W.C. Snyder, Z. Wan, Y. Zhang, and Y. Feng, "Thermal infrared (3-14 μm) bi-directional reflectance measurement of sands and soils, *Remote Sensing of Environment*, vol. 60, pp. 101-109, 1997.

[4] J.W. Salisbury, A. Wald, and D.M. D'Aria, "Thermal-infrared remote sensing and Kirchhoff's law, 1, Laboratory measurements", *Journal of Geophysical Research*, vol. 99, no. B6, pp. 11,897-11,911, 1994.

[5] A. Gillespie, S. Rokugawa, T. Matsunaga, J.S. Cothern, S. Hook, A.B. Kahle, "A temperature and emissivity separation algorithm for Advanced Spaceborne Thermal Emission and Reflection radiometer (ASTER) images", IEEE Transactions on Geoscience and Remote Sensing, vol. 36, pp.1113-1126, 1998.